

Supporting information

Manipulating the interfacial interactions of composite membrane via mussel-inspired approach toward enhanced separation selectivity

Jing Zhao,^{a,b} Chenhao Fang,^{a,b} Yiwei Zhu,^{a,b} Guangwei He,^{a,b} Fusheng Pan,^{a,b}

Zhongyi Jiang,^{*a,b} Peng Zhang,^{c,d} Xingzhong Cao^{c,d} and Baoyi Wang^{c,d}

^aKey Laboratory for Green Chemical Technology of Ministry of Education, School of Chemical Engineering and Technology, Tianjin University, Tianjin 300072, China.

^bCollaborative Innovation Center of Chemical Science and Engineering (Tianjin), Tianjin, 300072, China.

^cMulti-discipline Research Division, Institute of High Energy Physics, Chinese Academy of Sciences, Beijing 100049, China.

^dBeijing Engineering Research Center of Radiographic Techniques and Equipment, Beijing 100049, China.

1. Membrane photographs

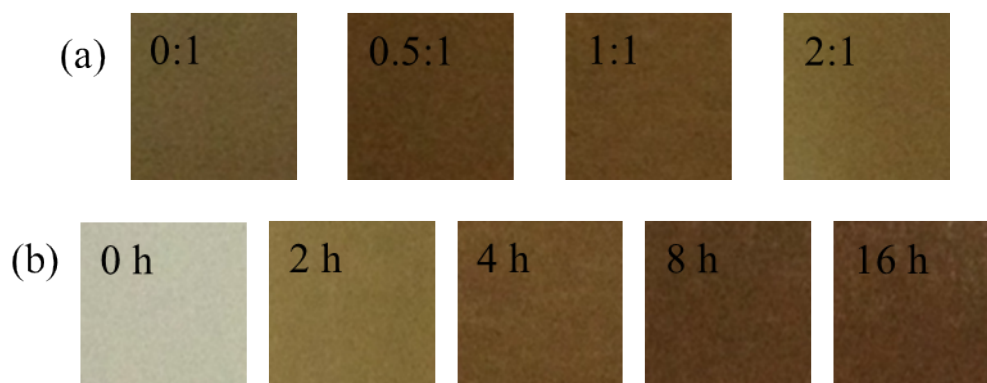


Fig. S1. The photographs of PEI-PDA/PAN membranes: (a) with different mass ratios of PEI/DA, (b) with different deposition times.

2. Morphology and chemical properties of membranes with different deposition times

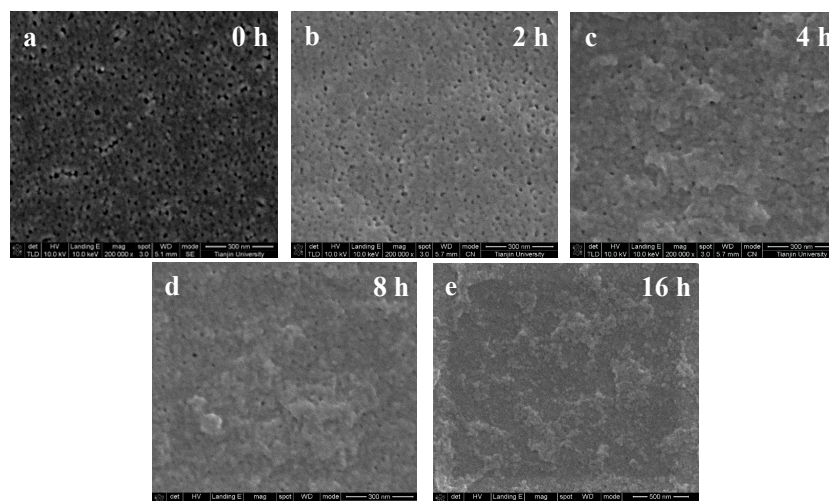


Fig. S2. FESEM images of membrane surface morphologies: (a) PAN, (b) PEI-PDA(2 h, 1:1)/PAN, (c) PEI-PDA(4 h, 1:1)/PAN, (d) PEI-PDA(8 h, 1:1)/PAN, (e) PEI-PDA(16 h, 1:1)/PAN

Fig. S2 shows the surface morphologies of PEI-PDA/PAN membranes with different deposition times. Due to the increased deposition amount of PEI-PDA with deposition time, the nanopores on PAN membrane are gradually covered, and the membrane colour changes from off white to dark brown (Fig. S1b). Furthermore, protuberances arising from the stacking and assembly of PEI-

PDA oligomers appear on membrane surface when the deposition time is longer than 4 h.

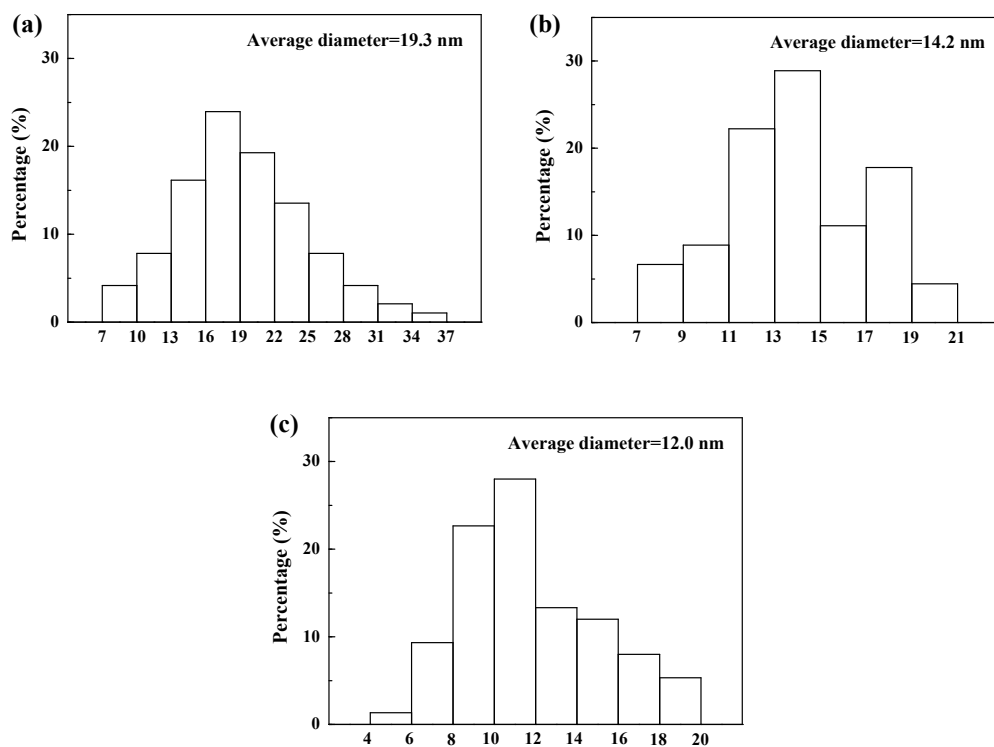


Fig. S3. Pore size distributions of (a) PAN membrane, (b) PDA/PAN membrane and (c) PEI-PDA/PAN membrane.

The pore size distributions of pristine and modified PAN membrane surfaces are obtained by measuring the nanopores on SEM images, as shown in Fig. S3. The average size of the nanopores on membrane surface decreases in the order of PAN membrane, PDA/PAN membrane and PEI-PDA/PAN membrane.

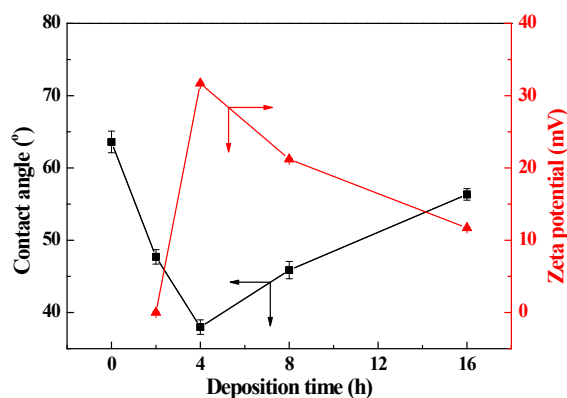


Fig. S4. Water contact angles and zeta potentials of SA/PEI-PDA(X, 1:1)/PAN membranes.

3. Interfacial interactions in SA/PAN and SA/PDA(4 h)/PAN membranes

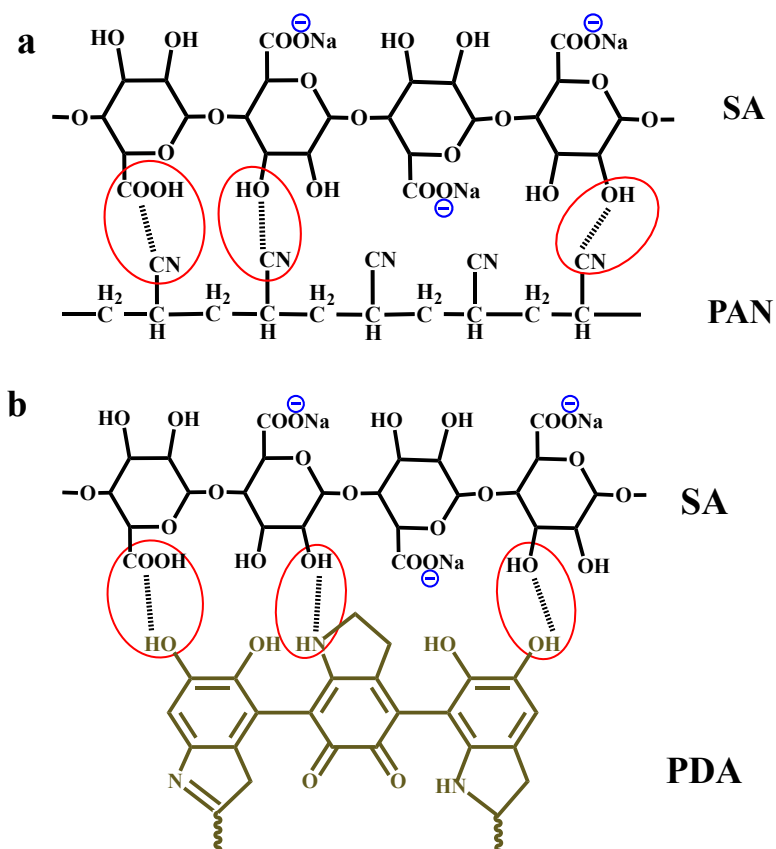


Fig. S5. Interfacial interactions in (a) SA/PAN and (b) SA/PDA(4 h)/PAN membranes.

4. Separation performance of pristine and modified PAN membranes

Table S1 Separation performance of pristine and modified PAN membranes.

Membrane	Permeation flux (kg/m ² h)	Separation factor
PAN	101	1
PDA(4 h)/PAN	34.3	1.6
PEI-PDA(4 h, 1:1)/PAN	7.28	5.5

5. Effect of temperature on membrane separation performance

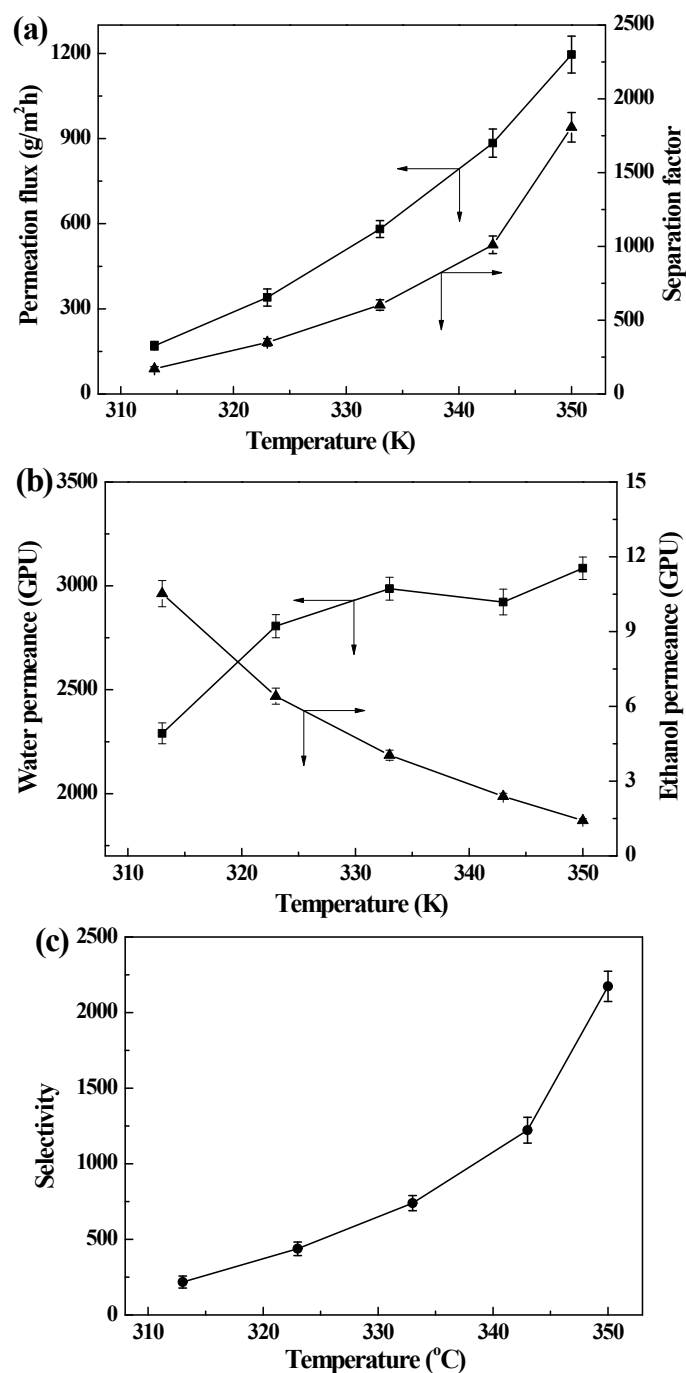


Fig. S6. The effect of temperature on the separation performance of SA/PEI-PDA(4 h, 1:1)/PAN membrane: (a) permeation flux and separation factor, (b) water/ethanol permeance, (c) selectivity

The pervaporation experiments of SA/PEI-PDA(4 h, 1:1)/PAN membrane under temperatures ranging from 313 to 350 K were performed with 90 wt% ethanol aqueous solution. It is shown in Fig. S6a that both the permeation flux and separation factor increase with operation temperature. In order to analyse the effects of operation

temperature on water/ethanol permeation process, water/ethanol permeance (driving force-normalized form of permeation flux, $(P/l)_i$, GPU) (1 GPU=7.501×10⁻¹² m³ (STP)/m² s Pa) and selectivity (β) were calculated as follows and shown in Fig. S6b and c.

$$(P/l)_i = \frac{J_i}{p_{i0} - p_{il}} = \frac{J_i}{\gamma_{i0}x_{i0}P_{i0}^{sat} - p_{il}} \quad (\text{S-1})$$

$$\beta = \frac{(P/l)_W}{(P/l)_E} \quad (\text{S-2})$$

where, J_i is the permeation flux of component i (g/(m² h)), l is the thickness of membrane (m), p_{i0} , p_{il} are the partial pressures of component i in the feed side and permeate side (Pa), p_{il} can be calculated approximately as 0 for the high vacuum degree in the permeate side. γ_{i0} and x_{i0} are the activity coefficient and mole fraction of component i in the feed liquid, respectively. P_{i0}^{sat} is the saturated vapor pressure of pure component i at operation temperature (Pa). The permeation flux of water and ethanol should be transformed into the volumes under standard temperature and pressure (STP): 1 kg of water vapor at STP = 1.245 m³ (STP), 1 kg of ethanol vapor at STP = 0.487 m³ (STP).¹

With the increase of temperature, water permeance continuously increases, while ethanol permeance exhibits a reverse tendency, thus resulting in the remarkable enhancement of selectivity. The impacts of temperature on water/ethanol permeation include three aspects: the loosened membrane structure at higher temperature results in lower diffusion resistance, favouring the water/ethanol permeation process; the molecule adsorption on membrane surface is suppressed, retarding the water/ethanol permeation process; the weakened coupling effect between water and ethanol inhibits the diffusion of ethanol along with water molecules, favouring water permeation and retarding ethanol permeation. For water permeation in SA/PEI-PDA(4 h, 1:1)/PAN membrane, the positive impacts on diffusion are dominant, which may be due to the high water affinity of membrane. By contrast, the negative impacts on adsorption and diffusion contribute more to ethanol permeation. The continuous enhancement of

water permeance and selectivity indicates that appropriately high operation temperature is advantageous for preferential permeation of water over ethanol.

6. Long-term separation performance

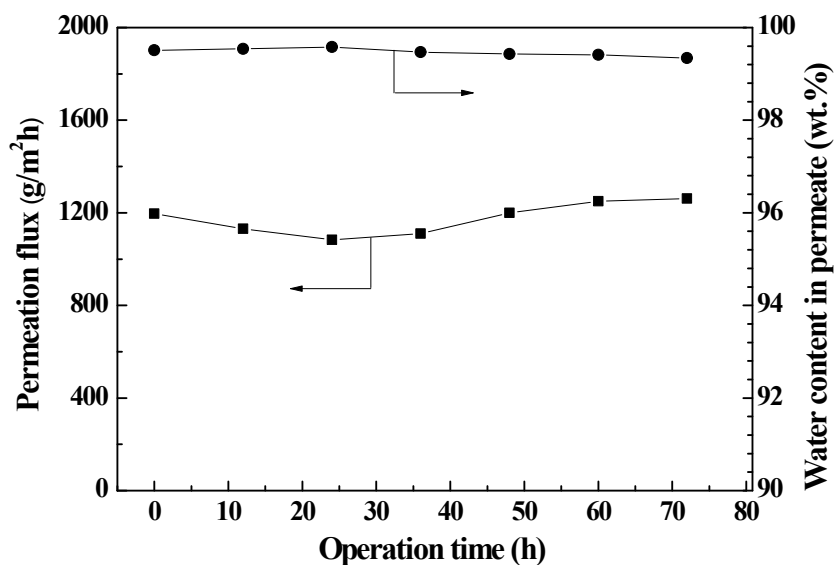


Fig. S7. The long-term separation performance of SA/PEI-PDA(4 h, 1:1)/PAN membrane

7. Comparison of membrane in this study with previous SA-based membranes in literatures

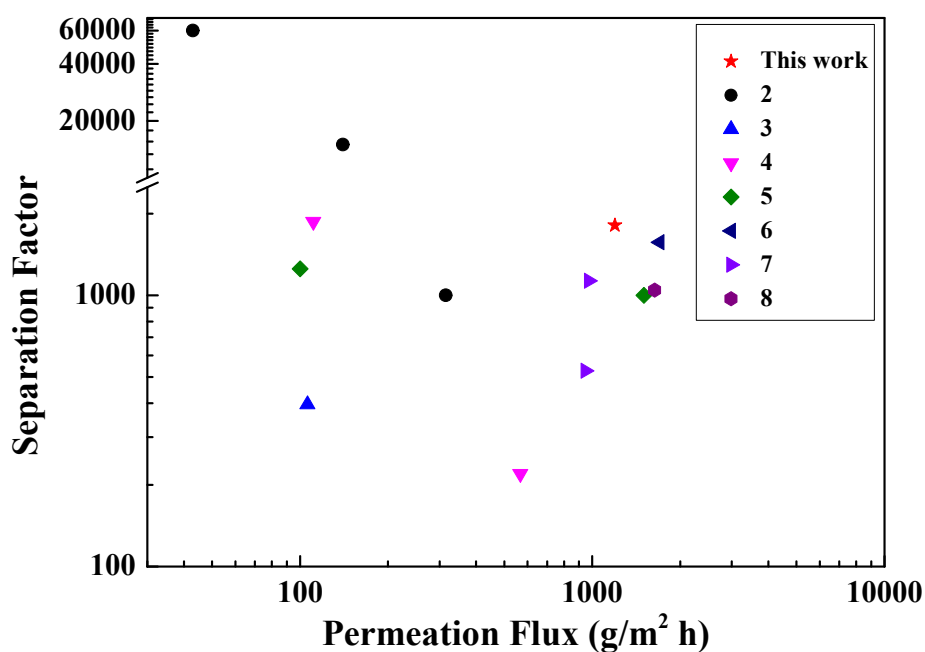


Fig. S8. Comparison of membrane in this study with previous SA-based membranes in literatures

References

1. B. P. Tripathi, M. Kumar, A. Saxena and V. K. Shahi, *J. Colloid Interface Sci.*, 2010, **346**, 54.
2. V. T. Magalad, A. R. Supale, S. P. Maradur, G. S. Gokavi and T. M. Aminabhavi, *Chem. Eng. J.*, 2010, **159**, 75-83.
3. F. U. Nigiz, H. Dogan and N. D. Hilmioglu, *Desalination*, 2012, **300**, 24-31.
4. S. G. Adoor, V. Rajineekanth, M. N. Nadagouda, K. C. Rao, D. D. Dionysiou and T. M. Aminabhavi, *Sep. Purif. Technol.*, 2013, **113**, 64-74.
5. V. T. Magalad, G. S. Gokavi, C. Ranganathaiah, M. H. Burshe, C. Han, D. D. Dionysiou, M. N. Nadagouda and T. M. Aminabhavi, *J. Membr. Sci.*, 2013, **430**, 321-329.
6. K. T. Cao, Z. Y. Jiang, J. Zhao, C. H. Zhao, C. Y. Gao, F. S. Pan, B. Y. Wang, X. Z. Cao and J. Yang, *J. Membr. Sci.*, 2014, **469**, 272-283.
7. C. Y. Gao, M. H. Zhang, J. W. Ding, F. S. Pan, Z. Y. Jiang, Y. F. Li and J. Zhao, *Carbohydr. Polym.*, 2014, **99**, 158-165.
8. C. H. Zhao, Z. Y. Jiang, J. Zhao, K. T. Cao, Q. Zhang and F. S. Pan, *Ind. Eng. Chem. Res.*, 2014, **53**, 1606-1616.